frontiers | Frontiers in Pharmacology

TYPE Systematic Review
PUBLISHED 26 September 2022
DOI 10.3389/fphar.2022.1025780

OPEN ACCESS

EDITED BY
Xiaojie Xu,
Beijing Institute of Technology, China

REVIEWED BY
Shuai Xu,
University of Jinan, China
Pan Wang,
North China University of Science and Technology, China
Xiaobo Wang,
Hubei University of Science and Technology, China
Chen Jianchao,
Shenyang Pharmaceutical University, China
Jinjun Shao,
Nanjing Tech University, China
Sherif Ashraf Fahmy,
American University in Cairo, Egypt

*CORRESPONDENCE
Yingqi Feng,
fengyingqivip@163.com

SPECIALTY SECTION
This article was submitted to Pharmacology of Anti-Cancer Drugs, a section of the journal Frontiers in Pharmacology

RECEIVED 23 August 2022
ACCEPTED 05 September 2022
PUBLISHED 26 September 2022

CITATION
Feng Y, Wu W and Li M (2022), Metal-organic frameworks for hepatocellular carcinoma therapy and mechanism. *Front. Pharmacol.* 13:1025780. doi: 10.3389/fphar.2022.1025780

Metal-organic frameworks for hepatocellular carcinoma therapy and mechanism

Yingqi Feng*, Wei Wu and Muzi Li

Beijing Key Laboratory for Green Catalysis and Separation, Department of Environmental Chemical Engineering, Beijing University of Technology, Beijing, China

In recent years, metal organic frameworks (MOFs) have attracted increasing attention in cancer therapy, because they can enhance the anticancer efficacy of photodynamic therapy (PDT), photothermal therapy (PTT), photoacoustic imaging, and drug delivery. Owing to stable chemical adjustability, MOFs can be used as carriers to provide excellent loading sites and protection for small-molecule drugs. In addition, MOFs can be used to combine with a variety of therapeutic drugs, including chemotherapeutics drugs, photosensitizers, and radiosensitizers, to efficiently deliver drugs to tumor tissue and achieve desired treatment. There is hardly any review regarding the application of MOFs in hepatocellular carcinoma. In this review, the design, structure, and potential applications of MOFs as nanoparticulate systems in the treatment of hepatocellular carcinoma are presented.

Systematic Review Registration: website, identifier registration number

KEYWORDS

hepatocellular carcinoma, MOFs, photothermal therapy, photodynamic therapy, chemodynamic therapy

Introduction

Hepatocellular carcinoma (HCC), a disease with a high incidence rate, will lead to 41,260 new diagnoses and 30,520 new deaths in the United States in 2022, according to the predictions of the National Cancer Institute. Accounting for 5% of all cancer deaths, the 5-year survival period for HCC is only 20.8%. Currently, surgery, radiotherapy, and chemotherapy based on targeted drugs are used to treat HCC (Chen et al., 2020; Rinaldi et al., 2021). Many patients with HCC do not have obvious symptoms, are usually diagnosed at an advanced stage, and are not suitable for surgery or transplantation (Du et al., 2021). Under the circumstances, chemotherapy, radiation therapy, and other treatment methods can effectively prolong the survival of patients and improve their quality of life (Yang et al., 2020; Zheng et al., 2021). However, chemotherapy or radiotherapy treatment faces many challenges, such as individual differences in HCC patients, poor sensitivity to chemotherapy or radiation therapy, and drug resistance (Mao et al., 2022). Furthermore, large doses of chemotherapy or radiotherapy can produce serious side effects, resulting in poor compliance of patients (Feng Y et al., 2020). Therefore, looking for new therapeutic methods with new mechanism, reducing the dose

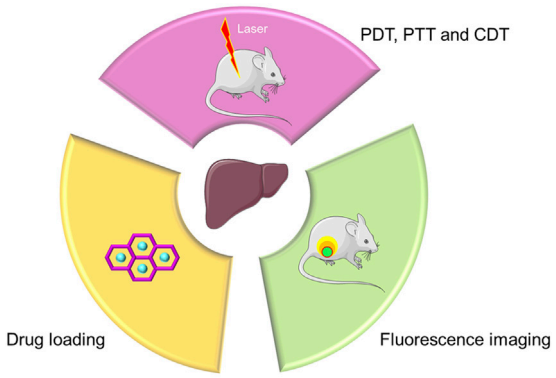

The schematic pieces were provided by Smart Medical Art and adapted (https://smart.servier.com).

GRAPHICAL ABSTRACT

of drugs, and maintaining antitumor efficacy are urgent problems that must be solved in the treatment of HCC (Hao Y.N et al., 2021; Philips et al., 2021).

Metal organic frameworks (MOFs) are a new form of coordination polymer developed in recent years, which are self-assembled involving metal ions and organic molecules. They have advantages such as porous structure, good biocompatibility, large specific surface area, and easy modification. They are widely used in the fields of catalysis (Sadeghi and Sillanpää, 2021; Zhang et al., 2021), energy storage (Downes and Marinescu, 2017; Jayaramulu et al., 2021), separation (Li T et al., 2022), and biomedicine (Carrillo-Carrión, 2020; Chen J et al., 2021). In cancer treatment, MOFs can enhance the anticancer effects of PDT, PTT, chemodynamic therapy (CDT), photoacoustic imaging, and drug delivery (Chen J et al., 2021). Additionally, MOFs have good chemical adjustability and can be used as carriers to provide excellent loading sites and protection for small-molecule drugs. MOFs can be combined with a variety of therapeutic drugs, including chemotherapeutics, photosensitizers (Luo et al., 2021; Zhao et al., 2021), and radiosensitizers, to efficiently deliver drugs to tumor sites (Osterrieth and Fairen-Jimenez, 2021) and achieve effective treatment (Carrillo-Carrión, 2020).

PDT is a novel tumor intervention approach that can replace traditional antitumor methods (Lakshmi and Kim, 2019). The mechanism of PDT produced by MOFs is to provide MOF molecules (photosensitizers) with specific structures such as porphyrins in tumor tissue and then locally irradiate the tumor with light of specific wavelength to excite the photosensitizer (Neufeld et al., 2021). The excited photosensitizer will transfer its energy and electron to the surrounding oxygen atoms, thereby generating singlet oxygen and other reactive oxygen species (ROS), and then kill tumor cells (Feng G et al., 2020; Chen D et al., 2021). Unlike chemotherapeutics and radiotherapy, which can cause systemic toxicity, oxygen substances produced during PDT treatment have no toxic effect on the body. Due to a series of advantages, such as noninvasive, small side effects, and accurate administration, PDT has been widely used in the treatment of superficial tumors and adjuvant treatment after surgical resection of tumors (Yu et al., 2020).

PTT, characterized by low systemic toxicity and efficient targeted local treatment, can ablate tumor cells with heat generated by a specific MOF after near-infrared (NIR) radiation. This approach is an extension of photodynamic therapy, in which a photosensitiser is excited with specific band light. This activation brings the sensitiser to an excited state where it then releases vibrational energy (heat) and kills the targeted cells (Xiong et al., 2021; Dai et al., 2022). Furthermore, the combination of PDT and PTT can synergistically improve antitumor efficacy and reduce side effects. The heat generated by PTT can improve blood flow and oxygen supply, thus improving the sensitivity of tumor cells to oxygen-dependent PDT. Furthermore, ROS produced by PDT can interfere with tumor physiology and change the microenvironment, thus improving the thermal sensitivity of tumor cells (Sun X et al., 2021; Zeng et al., 2021).

CDT is an effective strategy to inhibit tumor cells by converting H_2O_2 into highly toxic •OH through Fenton or Fenton-like reaction (Liu et al., 2021a). In the Fenton reaction generated by MOFs, Fe^{2+} in MOFs acts as a catalyst to convert H_2O_2 into highly toxic •OH. In addition to Fe^{2+}, generated Cu^{2+}, Mn^{2+}, and CO^{2+} can also catalyze the formation of •OH through Fenton-like reactions. In view of the characteristics of •OH produced during CDT, its combination with PDT can enhance the efficacy of PDT through the O_2 produced, and the production of highly toxic •OH can also kill cells with O_2, further inhibiting tumor cells. In recent years, PDT/CDT combination therapy has been methodically explored to enhance tumor oxidative stress and obtain better antitumor effect compared to monotherapy (Hao X et al., 2021; Tian et al., 2021).

Due to the advantages of the MOFs structure, several studies have attempted to utilize MOFs for anticancer applications. Such MOFs often are exploited for phototherapy, imaging effects, and drug loading functions. These studies have not only developed a variety of antitumor drugs with different structures but have also made remarkable achievements in drug delivery, loading and targeting (Lawson et al., 2021; Ma et al., 2021).

MOFs-mediated PDT, PTT and CDT treatment of HCC

Some MOFs with special structures can kill tumor cells through PDT, PTT or CDT effect. Therefore, MOFs have

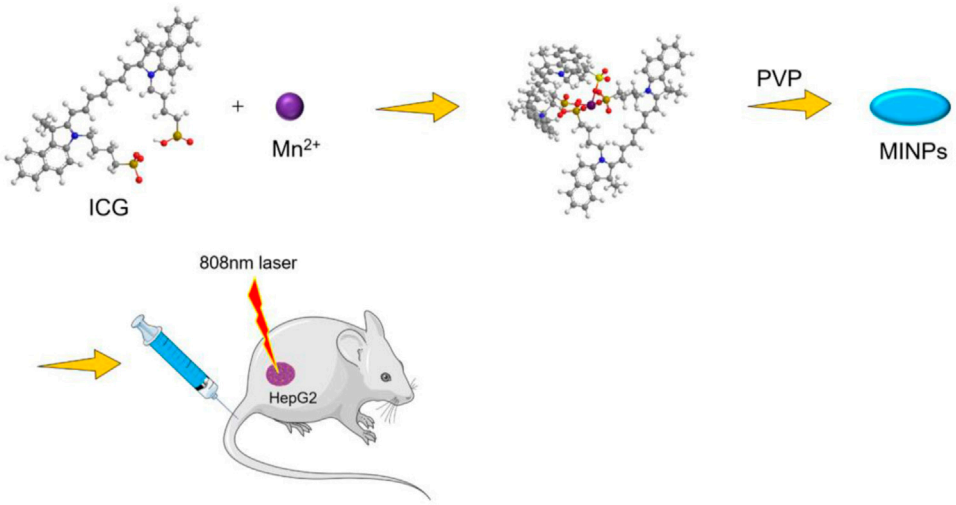

FIGURE 1
Synthesis and application of MINP. The schematic pieces were provided by Smart Medical Art and adapted [http://www.servier.com]. Servier Medical Art by Servier is licensed under a Creative Commons Attribution 3.0 Unported License.

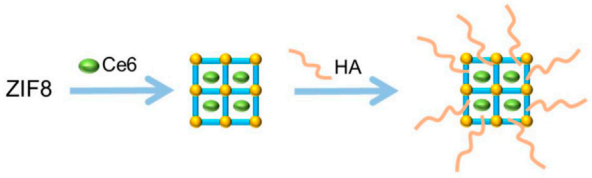

FIGURE 2
Synthesis of ZIF-8@Ce6–HA.

been applied in tumors treatment (Sun X et al., 2021; Wang et al., 2021; Zhou et al., 2021). Shi et al. (Shi et al., 2018) used a simple method to assemble Mn^{2+} and ICG and constructed new self-assembled nanoparticles (MINPs) under the protection of polyvinylpyrrolidone (PVP). *in vitro* experiments, under laser irradiation at 808 nm, MINPs achieved a clear inhibitory effect on HepG2 cancer cells (Figure 1). The MINPs solution was injected into the subcutaneous tumor model of mice, the photoacoustic (PA) signal around the tumor tissue during a 12-h period was recorded. The intensity of the PA signal obtained in the injection group was about three times higher than that of the control group (ICG administration group). After injection of MINPs, the positive signal of tumor magnetic resonance imaging (MRI) was enhanced and the average signal intensity gradually increased, indicating that MINPs achieved a time-dependent tumor accumulation. The quantitative detection results showed that the intensity of the MRI signal after 12 h of injection was 1.8 times higher than before injection. The results of *in vitro* PTT treatment and *in vivo* imaging revealed that cell necrosis and tumor damage could be observed in the tumor (HepG2 cells) treated by MINPs, while the control group did not present any obvious tumor damage. These experiments indicated that MINPs could be expected to become a highly effective PTT therapeutic drug and could be applied for imaging-guided PTT of HCC.

Fu et al. (2020) developed a new therapeutic agent ZIF-8@Ce6-HA using a one-step method. In this therapeutic agent, ZIF-8 was loaded with Chlorin E6 (CE6) and then modified with hyaluronic acid (HA) ZIF-8@Ce6-HA exhibited a good encapsulation rate, cell absorption, and biocompatibility. Mass spectrometry test data showed that HA modification prolonged the blood circulation time of these particles and decreased toxicity (Figure 2). *In vitro* anticancer experiments showed that after 5 min of irradiation at 660 nm, free CE6 exhibited slight cytotoxicity at a higher concentration (3 mM), and approximately 29.5% of HepG2 cells died due to ROS generated by PDT. Free CE6 molecules tend to agglomerate in the aqueous phase to reduce the efficiency of PDT, while ZIF-8@Ce6-HA overcomes this problem. The ZIF-8@Ce6-HA group showed greater cytotoxicity than the free CE6 group after irradiation with death of all cancer cells (88.4%). That study innovatively introduces a new therapeutic agent CE6 for PDT.

Liu et al. (2017) constructed MOFs with biocompatible Zr ions and Meso-Tetra (4-carboxyphenyl) porphine (TCPP), then loaded doxorubicin (DOX) to build a new nanoparticle (NP), DOX@NPMOF. The content of DOX loaded on the particles was as high as 109%. In an *in vitro* HepG2 cell model, DOX@NPMOF administration with a 655 nm laser showed good inhibitory ability (IC_{50} = 67.72 μg/ml) and the lethality of HepG2 cells

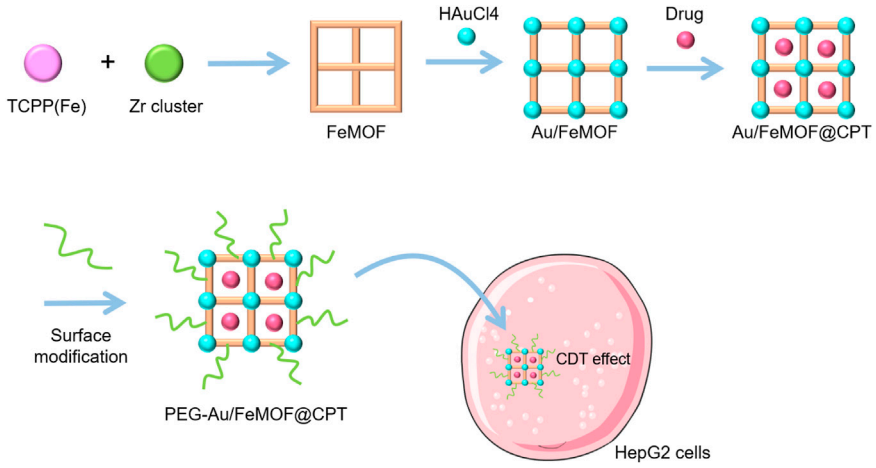

FIGURE 3
Synthesis and application of PEG-Au/FeMOF@CPT NPs. The schematic pieces were provided by Smart Medical Art and adapted [http://www.servier.com]. Servier Medical Art by Servier is licensed under a Creative Commons Attribution 3.0 Unported License.

was as high as 90%. Subsequently, a mouse subcutaneous tumor model was used to investigate the anticancer effect of DOX@NPMOF. The experiment was divided into four groups, namely, the saline group, the PDT treatment group, the chemotherapy group, and the combined treatment group (DOX@NPMOF), to compare the results. First, the fluorescence intensity of the cancer area was recorded by imaging. After the accumulation of NPMOF reached its maximum, the tumor tissues of mice in each group were irradiated with a 655 nm laser (180 J/cm^2) for 15 min. Subsequently, the size of the tumor in different groups was monitored. The experimental results showed that the combined treatment group achieved the best effect. After 2 days of treatment, the tumors of mice were significantly reduced and gradually completely eradicated. The effects obtained were superior to that of the chemotherapy group and the PDT treatment group, and no skin/tissue damage was observed in any mice.

Ding et al. (2020) constructed FeMOFs nanoparticles (NPs) with TCPP (Fe) and zirconium clusters, then loaded the hydrophobic chemotherapeutic drug camptothecin (CPT), and *in situ,* grew small gold (Au) NPs on its surface to gain novel NPs PEG-Au/FeMOF@CPT NPs. The Au NPs externally anchored were further modified by 1-dodecyl mercaptan ($C_{12}SH$) and methoxypolyethylene glycol mercaptan (PEG-SH) (Figure 3). The MTT assay was used to evaluate the anticancer effects of CDT on HepG2 cells. The half maximum inhibitory concentration (IC_{50}) of CPT monotherapy was 206 ± 22 μg/ml. Although the amount encapsulated in CPT was only 7.7%, the IC_{50} value of the chemokinetic treatment group (PEG-Au/FeMOF-NPs) still reached 3.51 ± 0.26 μg/ml. Conversely, the IC_{50} value of the combined chemotherapy and chemokinetic treatment group (PEG-Au/FeMOF@CPT NPs) was the lowest (0.31 ± 0.04 μg/ml). This indicates that the combination of CDT and CPT may achieve a good synergistic activity and can effectively inhibit tumor growth.

MOFs for synergistic cancer treatment

Chemotherapy, one of the main methods for treating tumors, uses chemical synthetic drugs to kill cancer cells. Some chemotherapeutic drugs, such as DOX and CPT can be combined with MOFs to overcome the problems of poor drug release, side effects of systemic administration, and drug resistance, to enhance the antitumor effect. MOFs achieve high drug loading by changing the binding sites and porosity, promoting accumulation in the tumor, and prolonging the drug release by appropriate modification. Therefore, MOFs achieve good synergistic effects with chemotherapy drugs to achieve antitumor goals.

Xiao et al. (2020) designed a biomimetic MOF particle (CDZ) loaded with dihydroartemisinin (DHA) based on the ZIF-8 structure. They first prepared Fe^{2+} doped ZIF-8 NPs using a simple method and loaded DHA into the NPs to form DZs. The DZs were then inserted into the shell prepared with cancer cell membrane to obtain CDZs, which able to accumulate and be released into the tumor tissue. When Fe^{2+} in particles combine with DHA, the hydrogen peroxide bridge will fracture reductively and oxygen center free radicals will be generated, which will lead to rearrangement of carbon center free radicals and induce DHA toxicity. DHA influences the mitochondrial-dependent apoptosis pathway and can inhibit the activation of the nuclear factor kB (NF-kB) signaling pathway, thus promoting tumor cell apoptosis (Figure 4).

In vivo antitumor effects of CDZs were evaluated in a mouse subcutaneous tumor model. In this experiment, tumors in both

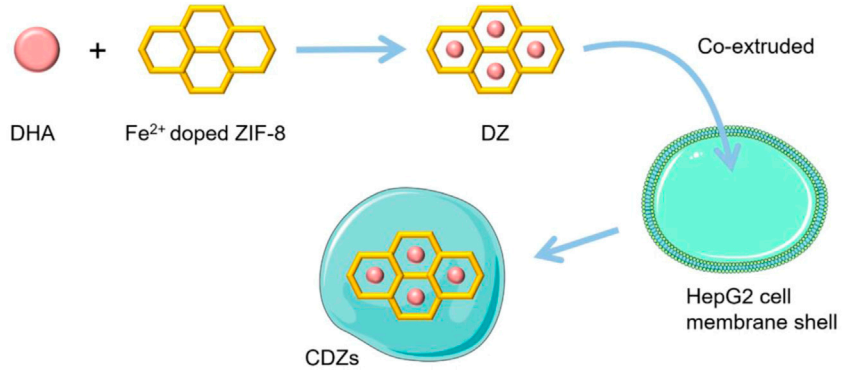

FIGURE 4
Synthesis and application of CDZs. The schematic pieces were provided by Smart Medical Art and adapted [http://www.servier.com]. Servier Medical Art by Servier is licensed under a Creative Commons Attribution 3.0 Unported License.

the normal saline group and the Fe/ZIF-8 (CZ) treatment group showed similar growth without inhibition. Treatment with DZs resulted in a 56.9% reduction in tumor volume, while a significant 90.8% reduction in tumor volume was observed after treatment with CDZ. Thus, CDZs had a marked anti-HCC effect and the efficacy of CDZs was significantly superior to that of DZS. The homogeneous aggregation of NPs induced by the cell membrane and the improvement of the stability of the NPs minimize drug loss and promote the antitumor efficacy of CDZs.

Fytory et al. (2021) constructed new types of MOFs based on Zr ion and UiO-66- NH_2, which loaded DOX, and their surfaces were successively modified with folic acid (FA), lactonic acid (LA) and glycyrrhetinic acid (GA). Compared to the control group, treatment of HepG2 cells with DOX loaded in NMOF could stimulate cell death. The apoptosis rates of the single-ligation group (LA) and the double-ligation group (LA+GA) were 30.1% and 29%, respectively. The *in vitro* inhibitory activity experiment in HepG2 cells showed that the inhibitory ability (IC_{50}) of the free DOX group, the NMOF group, the FA-NMOF group, the LA-NMOF group, the GA-NMOF group and the LA-GA-NMOF group were 1.200, 5.982, 1.887, 0.641, 0.986, and 0.520 μM, respectively. The experiment showed that the apoptosis rate of HepG2 cells induced by double ligation NMOF was higher than in the DOX treatment group. The results of this study further demonstrated the superiority of dual connectivity NMOFs as a drug delivery system for the treatment of HCC.

Liu et al. (2022) developed a multifunctional DOX loading NPs UiO-66/Bi_2S_3@DOX using a one-step solvothermal method, the particle could simultaneously achieve a photothermal effect and pH-triggered DOX release. The combination of transcatheter arterial chemoembolization (TACE) and PTT significantly inhibited tumor growth. Histopathological analysis showed extensive necrosis, decreased regulation of angiogenesis, and increased apoptosis in treated HCC. These results indicate that the nanosystem platform UiO-66/Bi_2S_3@DOX is a promising therapeutic agent to improve the TACE treatment of HCC.

The anticancer properties of UiO-66/Bi_2S_3@DOX were investigated in N1S1 tumor-bearing rats. MRI showed that there were no significant differences in preoperative tumor volume among seven treatment groups (total of 55 rats) in the study. On day 10 after the operation, the tumor volumes in the phosphate buffered saline solution (PBS), PBS+NIR, DOX, UiO-66/Bi_2S_3, UiO-66/Bi_2S_3@DOX, UiO-66/Bi_2S_3+NIR, and UiO-66/Bi_2S_3@DOX+NIR treatment groups were 8136 ± 799.5, 8043 ± 736.0, 4740 ± 954.9, 8461 ± 788.5, 4729 ± 658.3.0, 5219 ± 770.5, and 2826 ± 842.3 mm^3, respectively. The tumor growth rate in the PBS group, the PBS+NIR group, and the UiO-66/Bi_2S_3 group on day 10 was higher than in the other four treatment groups, showing a poor inhibitory capacity of tumor volume. There were no significant differences between the DOX, UiO-66/Bi_2S_3@DOX, and the UiO-66/Bi_2S_3+NIR group, but tumor suppression in the UiO-66/Bi_2S_3@DOX+NIR group was significantly better than any other group. Moreover, compared to other groups, the average tumor weight in the UiO-66/Bi_2S_3@DOX+NIR group was the lowest, further demonstrating that the combination achieved better tumor inhibition. In conclusion, this *in vivo* antitumor study confirmed that simultaneous PTT and chemotherapy produce synergistic enhancement effects that cannot be achieved with a single treatment approach.

Samui et al. (2019) developed a NH_2-MIL-53(Al)NMOF modified with LA and loaded with DOX. HepG2 cell line has high expression of the asialoglycoprotein receptor (ASGPR), and LA has strong binding affinity to this receptor, thus NMOF modified with LA achieves better anti-HCC activity. In their study, MTT analysis showed that NH_2-MIL-53(Al)NMOF achieved stronger cytotoxicity against the HepG2 cell line compared to the normal cell line.

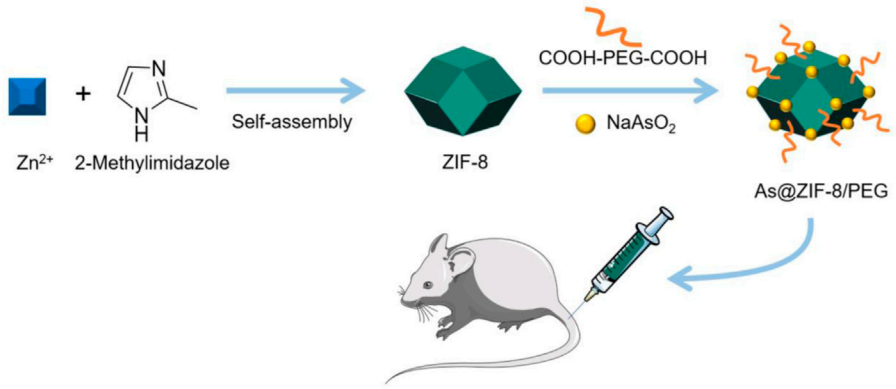

FIGURE 5
Synthesis and application of As@ZIF-8/PEG NPs. The schematic pieces were provided by Smart Medical Art and adapted [http://www.servier.com]. Servier Medical Art by Servier is licensed under a Creative Commons Attribution 3.0 Unported License.

In another study, Chen et al. (2022) used ZIF-8 as the backbone and loaded with arsenic trioxide (ATO) to develop the NPs As@ZIF-8. These NPs were then encapsulated in COOH-PEG-COOH to obtain As@ZIF-8/PEG NPs, which improved their pharmacokinetic properties (Figure 5). A mouse subcutaneous tumor model was used to test the activity of As@ZIF-8/PEG. Mice were randomly divided into four groups (five mice in each group) until tumors grew to 200–400 mm^3. The first group was the control group with only insufficient radiofrequency ablation (IRFA) treatment. The second group was treated with IRFA and free ATO. The third group was treated with IRFA+As@ZIF-8/PEG NPs and the fourth group with IRFA+ZIF-8 NPs. The tumor growth curve shows that the inhibitory effect of the As@ZIF-8/PEG NPs-treated group on residual tumor growth was the most obvious, while that of the ZIF-8 nanocarrier was almost negligible. It should be noted that ATO also partially delayed tumor growth, but the antitumor effect of ATO was lower than that of the control group As@ZIF-8/PEG NP. The anatomical image of the tumor tissue on day 21 showed that the tumor volume in the As@ZIF-8/PEG NP group was lower than in the other groups, and the tumor volume of the free ATO group was lower than that of the control group, but much larger than that of the As@ZIF-8/PEG NP group. This experiment indicated that As@ZIF-8/PEG NPs combined with IRFA could significantly improve the therapeutic effects of IRFA.

Cheng et al. (2019) prepared magnetic nanocomposite Fe_3O_4-ZIF-8 carrying DOX for the treatment of HCC. The Cell Counting Kit-8 (CCK-8) assay and flow cytometry were used to determine the inhibitory effects of Fe_3O_4-ZIF-8, DOX and DOX@Fe_3O_4-ZIF-8 on MHCC97H cells. The results of the CCK-8 assay showed that Fe_3O_4-ZIF-8 was not toxic to MHCC97H cells, DOX@Fe_3O_4-ZIF-8 had an obvious inhibitory effect on MHCC97H cells. The cell uptake test showed that DOX@Fe_3O_4-ZIF-8 accumulated in the cytoplasm and nucleus, possibly because nanoscale DOX@Fe_3O_4-ZIF-8 can easily cross the cell membrane. Furthermore, due to effective drug accumulation, DOX@Fe_3O_4-ZIF-8 can induce apoptosis of MHCC97H cells. In sum, compared to free DOX, DOX@Fe_3O_4-ZIF-8 had a stronger effect on HCC cells, indicating that it has the potential to become a chemotherapeutic drug for HCC.

Li Z et al. (2022) developed a triptolide (TPL)-loaded MOF (TPL@CD-MOF) based on the cyclodextrin (CD) structure, which improves the solubility and bioavailability of TPL, thus enhancing its inhibitory effect on HCC. In the Huh-7 subcutaneous xenograft tumor model, the antitumor activity of TPL@CD-MOF was investigated. The results showed that compared to the normal saline group or the free TPL group, the TPL@CD-MOF group produced better antitumor efficacy and the tumor volume and tumor weight of this group were lower.

Bieniek et al. (2021) prepared a pocket wheel framework (PPF) based on Zn $(NO_3)_2$•$6H_2O$ and TCPP and loaded it with sorafenib (SOR) to obtain SOR@PPF. In different proportions of ethanol aqueous solutions, SOR was deposited on PPF in two different sizes with different resolution rates, i.e., slow released (SR) and fast released (FA). In the *in vitro* anti-HCC cell activity assay, the concentration for 50% of maximal effect (EC_{50}) of SOR alone was 13.8 μM and 10.0 mM after 24- and 72-h administration, respectively. In contrast, the EC_{50} of SOR@PPF was 1.6 μM and 1.81 μM after 24 and 72 h of administration, respectively. In *in vivo* experiments, compared to the control group, both SR-SOR@PPF and FR-SOR@PPF effectively inhibited distant metastasis and *in situ* cancer recurrence after operation. Compared to the control group, in rats treated with SR-SOR@PPF, the odds ratios (OR) of distant metastasis and *in situ* recurrence were 0.26 and 0.38, respectively. In the rats treated with FR-SOR@PPF, the OR values of distant metastasis and *in situ* recurrence were 0.56 and

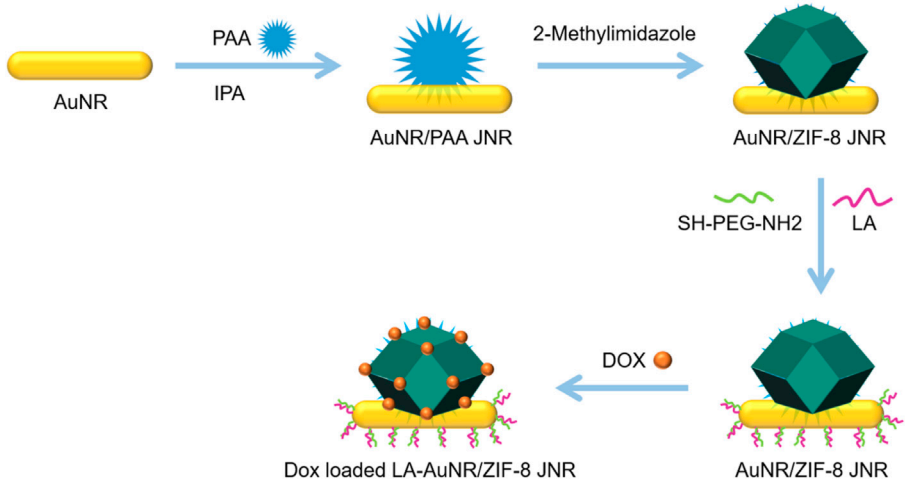

FIGURE 6
Synthesis of NPsLA-AuNR/ZIF-8 JNPs.

0.63, respectively. These results indicated that the antitumor effect of SOR@PPF improved significantly compared to free SOR. In addition, by controlling PPF degradation and sorption, the antitumor effect of SOR *in vitro* and *in vivo* can be regulated.

Zhang et al. (2021) mixed one-dimensional Au nanorod (AuNR) with PAA, aqueous ammonium hydroxide solution ($NH_3 \bullet H_2O$), and isopropanol (IPA) to obtain AuNR/PAA JNPs. Zinc nitrate and imidazole (Hmim) were then added to form ZIF-8 on the PAA side of AuNR/PAA JNPs and AuNR/ZIF-8 JNPs were obtained. Finally, the exposed side surface of AuNR was modified with LA to obtain the LA-AuNR/ZIF-8 JNPs targeting HCC (Figure 6). These NPs could load about 30 wt% DOX and achieved better and faster drug release under the NIR laser and pH 5.3. *In vivo* studies using mice xenografted with H-22 tumor cells showed that the JNPs+laser group (808 nm) caused more cancer cell death than the pure JNPs group, which indicated that JNP could act as a photothermal agent to effectively kill cancer cells under NIR laser irradiation. The tumor inhibition rate of the JNP+DOX+laser group was as high as 93%, which was higher than that of the JNP+DOX and JNP+laser groups. These findings indicated that LA-AuNR/ZIF-8 JNPs, combined with drugs and lasers, could cause synergistic chemotherapy and PTT effects, thus achieving better therapeutic effects.

Liu et al. (2021b) loaded the ferroptosis inducer SOR, which is used to treat advanced HCC, onto the Fe metal organic framework [MIL-101 (FE)] to prepare MIL-101(Fe) @SOR NP. After 60 h of administration, the drug release of these NPs reached approximately 35% at pH 5.5 and only 10% at pH 7.4. These NPs significantly induced ferroptosis in

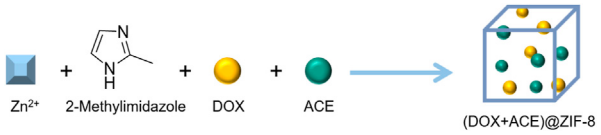

FIGURE 7
Synthesis of (DOX+ACE)@ZIF-8.

HepG2 cells and decreased the concentration of glutathione and glutathione peroxidase 4 (GPx-4). The results of *in vivo* experiments showed that MIL-101(Fe)@SOR NPs could significantly inhibit tumor progression, reduce the expression level of GPx-4, and the long-term toxicity was negligible. Subsequently, to enhance the nanodrug tumor targeting and penetration capabilities, an iRGD peptide (amino acid sequence: CRGDK/RGPD/EC) was introduced containing a tumor-homing motif (RGD) and a tissue penetration motif (CendR).

In vivo, mice with implanted H-22 tumor cells exhibited extremely rapid tumor growth in the control group and MIL-101(Fe) NPs group, while in other groups, the growth was slow. In the MIL-101(Fe)@SOR+iRGD group, the tumor was the smallest. Compared to other groups, mice treated with MIL-101(Fe)@SOR+iRGD had the highest tumor inhibition and significantly reduced tumor weight. Additionally, during the treatment period, the weight of the mice in the MIL-101(Fe) @SOR+iRGD group did not decrease significantly. Tumor sections were stained and imaged to compare with other groups, the necrosis area of tumor tissue in the MIL-101 (Fe) @SOR+iRGD group was the largest, and the number of GPX-4

positive cells was the lowest. These experimental results show that MIL-101(Fe)@SOR+iRGD has relatively optimal tumor inhibition.

Jing et al. (2021) prepared a nanocarrier zeolite imidazoline framework (ZIF-8) by the one-pot method and loaded DOX and acetazolamide (ACE) simultaneously to obtain (DOX+ ACE)@ZIF-8. The DOX and ACE drug loading efficiencies were 7.29% and 4.62%, respectively (Figure 7). *In vitro* cell inhibitory activity experiments showed that the inhibitory rate (IC_{50}) of blank ZIF-8 in the human normal liver cell line HL7702 was greater than 100 μg/ml, which indicates that the cytotoxicity of ZIF-8 is low. The antitumor effect of (DOX+ACE)@ZIF-8 was dose dependent and the inhibitory capacity (IC_{50}) against Walker 256 cells was 2.36 μG/ml and 0.66 μG/ml (corresponding to ace and DOX), respectively. The safety of (DOX+ACE)@ZIF-8 *in vivo* was experimentally evaluated. The hemolytic potential of (DOX+ACE)@ZIF-8 in 50–200 μG/ml is negligible (<5%). Rats injected with (DOX+ACE)@ZIF-8 by a single intratumoral dose or intravenous injection showed little damage to normal tissues or adverse hematological effects, which preliminarily demonstrated the high biocompatibility of (DOX+ACE)@ZIF-8.

Application of MOF in tumor imaging

Some MOFs have specific photosensitive properties and can shine under excitation at a specific wavelength, enabling MOFs to possess the ability of tumor imaging, which is a very important property in identifying and treating tumors (He et al., 2019; Huang et al., 2021).

Sun et al. (Sun Q.X et al., 2021) prepared MOF-RB by loading rhodamine B (RB) into a common MOF structural unit UiO-66-NH_2 (Zr-MOF). MOF-RB was used to perform confocal laser scanning microscopy (CLSM) fluorescence imaging and

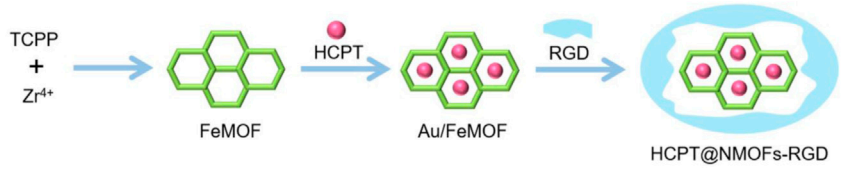

FIGURE 8
Synthesis of HCPT@NMOFs-RGD.

TABLE 1 Key characteristics of the MOFs involved in this article.

MOFs	Metal	Component	Drug	Surface functionalization	Ref
MINPs	Mn^{2+}	porphyrin, ICG	—	—	Shi et al. (2018)
ZIF-8@Ce6–HA	Zn^{2+}	2-Methylimidazole	Ce6	HA	Fu et al. (2020)
DOX@NPMOF	Zr^{2+}	TCPP	DOX	—	Liu et al. (2017)
PEG-Au/FeMOF@CPT	Zr^{2+}	TCPP	CPT	Au NPs,C_{12}SH,PEG-SH	Ding et al. (2020)
CDZs	Fe^{2+}, Zn^{2+}	2-Methylimidazole	DHA	Cancer cell membrane	Xiao et al. (2020)
LA-GA-NMOF	Zr^{4+}	UiO-66-NH_2	DOX	FA, LA, GA	Fytory et al. (2021)
UiO-66/Bi_2S_3@DOX	Bi^{3+}	UiO-66	DOX	—	Liu et al. (2022)
NH2-MIL-53(Al)NMOF	Al^{3+}	2-Aminoterephthalic acid	DOX	LA	Samui et al. (2019)
As@ZIF-8/PEG	Zn^{2+}	2-Methylimidazole	ATO	COOH-PEG-COOH	Chen et al. (2022)
DOX@Fe_3O_4-ZIF-8	Fe^{2+}, Zn^{2+}	2-Methylimidazole	DOX	—	Cheng et al. (2019)
TPL@CD-MOF	K^{+}	CD	TPL	—	Li Z et al. (2022)
SOR@PPF	Zn^{2+}	TCPP	SOR	—	Bieniek et al. (2021)
LA-AuNR/ZIF-8	Zn^{2+}	2-Methylimidazole	DOX	Au nanorod, LA	Zhang H et al. (2019)
MIL-101(Fe)@SOR	Fe^{3+}	2-Aminoterephthalic acid	SOR	—	Liu et al. (2021b)
(DOX+ACE)@ZIF-8	Zn^{2+}	2-Methylimidazole	DOX, ACE	—	Jing et al. (2021)
MOF-RB	Zr^{2+}	UiO-66-NH_2	RB	—	Sun Q.X et al. (2021)
HCPT@NMOFs-RGD	Zr^{4+}	TCPP	HCPT	RGD peptide	Shang et al. (2022)
FA-NPMOF	Gd^{3+}	TCPP	FA	—	Chen et al. (2019)

inductively coupled plasma mass spectrometry (LA-ICPMS) laser ablation under elemental imaging on the same group of HepG2 cells in the designated area. This dual-mode imaging strategy helps visualize the migration of copper transporter 1 (CTR1), while providing clear information on the migration and redistribution of CTR1 during exposure to divalent copper/cisplatin through joint imaging of CLSM and LA-ICPMS on the same group of HepG2 cells. This dual-mode imaging strategy provides extremely valuable information to elucidate biological processes related to CTR1.

Shang et al. (2022) prepared a zirconium porphyrin metal organic framework (NMOFs) and then loaded 10-hydroxycamptothecin (HCPT) into the pores of the NMOFs and wrapped it with arginine glycine aspartic acid (RGD) peptide to obtain a new nanocomposite HCPT@NMOFs-RGD (Figure 8). In a mouse tumor model with xenograft, the antitumor activity of HCPT@NMOFs-RGD was evaluated. NMOFs-RGDs had low toxicity, good biocompatibility, and strong imaging ability. In a zebrafish HCC model, specific binding of HCPT@NMOFs-RGD with the integrin $\alpha_v\beta_3$ and enrichment in tumors lead to a reduction in tumor volume. In the mouse xenograft tumor model, after 12 days of HCPT@NMOFs-RGD treatment, the tumor size of the NMOFs group (PDT treatment) and the HCPT group (chemotherapy) was smaller than that of the blank control group. Importantly, tumors in the HCPT@NMOFs-RGD group were significantly reduced and even disappeared in one sample. Tumor weights in the NMOF group, the HCPT group, and HCPT@NMOFs-RGD all decreased significantly. These data prove the advantage of synergistic antitumor of HCPT@NMOFs-RGD.

Chen et al. (2019) synthesized a new type of NPs, namely, folic acid nanoscale gadolinium porphyrin metal organic frameworks (FA-NPMOF), based on a gadolinium porphyrin-based MOF and then combined with folic acid (FA). Subsequently, the biological toxicity and imaging ability of FA-NPMOF were measured using HepG2 cells, zebrafish embryos and larvae. *In vitro* cell experiments, HepG2 cells were found to have significant apoptosis after treatment with PDT (655 nm) with FA-NPMOF. In *in vivo* experiments in zebrafish, HCC cells were necrotic and triggered inflammatory reactions. However, enhanced green fluorescent protein (EGFP) fluorescence, thermal imaging, and tumor shrinkage also verified its therapeutic effect. These experiments showed that FA-NPMOF achieved a good therapeutic effect on HCC *in vitro* and *in vivo*. The key information of the MOFs mentioned above is listed in Table 1.

Challenges of MOF in cancer treatment

Although theoretically a variety of metal ions can be used in MOF assembly, in fact—after excluding toxic metal ions—only a few ions are suitable; these include Zr (Wang et al., 2021), Fe (Wang et al., 2019; Yao et al., 2022), Zn (Farhadi et al., 2021; Wan et al., 2021), Mn (Lan et al., 2018; Li et al., 2018), and Cu (Lan et al., 2018; Li et al., 2018), which limits the diversification of MOFs types. In addition to the limitation of the metal ion type, the cytotoxicity caused by the physicochemical properties of the MOFs is also an important factor limiting the application of MOFs (Xia et al., 2021; Xie et al., 2021). These key physicochemical properties, including size distribution, shape, and surface hydrophobicity, affect the solubility of MOFs. To overcome these problems, a large number of studies have been carried out in recent years to modify the surface of MOFs with hydrophilic groups or prepare MOFs as liposomes (Zhang D et al., 2019; Bao et al., 2020; Wang et al., 2021). These works are of great practical value.

Another problem that restricts the use of MOFs in anti-HCC treatment is drug loading and drug release (Gharehdaghi et al., 2021; Jiang et al., 2021). The drug loading and release properties of these nanodrug delivery platforms depend on both the structure of the MOFs and the properties of the loaded drugs. It is challenging to overcome this dilemma. The structure of MOFs needs to be chemically modified according to the different types of loaded drug to match the carrier and drug and achieve a more suitable dissolution. MOFs have a large molecular weight, and *in vivo* metabolic limitations resulting from mass drug administration are also a problem worthy of follow-up research (Lakshmi and Kim, 2019; Chen J et al., 2021).

Conclusion

The application of MOFs in breast cancer (Qin et al., 2020; Xu et al., 2020; Alves et al., 2021; Zhou et al., 2021) and cervical cancer (Sava Gallis et al., 2017; Zhao et al., 2018; Rao et al., 2022) is relatively mature, while in HCC it is still in its infancy. This is mainly because the pathogenesis of HCC is complex and there are less drugs available for HCC treatment. In this paper, we reviewed the latest progress of MOFs in HCC therapy, including the latest research progress in direct use of MOFs as anti-HCC treatment and in combination with other drugs. As a porous material, the MOF not only has photodynamic and photothermal properties but also has the advantages of high porosity, adjustable structure, versatility, and biocompatibility. Through synergistic treatment of photodynamic and photothermal effects, MOFs has shown outstanding effects in various solid tumor treatment. On the basis of the macroporous structure of the MOFs, chemotherapy drugs such as DOX, CPT, and SOR have been used to construct drug-loaded NPs with MOFs to cooperate with photodynamic, photothermal, chemical dynamics, and other methods to treat HCC. According to the reported cases, ZIF-8, UiO-66 and porphyrin MOFs are the most common materials. Porphyrin MOFs possess PDT and PTT effects, while MOFs such as ZIF -8 and UiO-66 mainly be used as the drug delivery platform to HCC treatment.

In HCC chemotherapy, the most problem is drug resistance and toxicity caused by excessive administration. MOFs can be administered through TACE technology to create new possibilities of local drug delivery and controlled release, while avoiding the toxicity of chemotherapeutics drugs. In addition, the new therapeutic mechanisms of PDT, PTT and CDT can resolve the problem of drug resistance. It is hoped that some stimuli-responsive (pH, sound and thermal) MOFs will be applied to HCC treatment in the future, so as to diversified treatment strategies. Most of the reported MOFs are constructed with known ligand structures because the application of MOFs is still in the exploratory stage. With further research, more advanced structures will be used to construct different MOFs. It is expected that these new developments will bring a new situation to HCC treatment.

Data availability statement

The original contributions presented in the study are included in the article/supplementary material, further inquiries can be directed to the corresponding author.

Author contributions

YF and WW designed and supervised the review, YF and WW collected, analyzed, and drafted the main manuscript; YF, WW, and ML checked references, figures and tables; YF revised the manuscript. All authors have read and approved the final version.

Funding

This study was supported by the Beijing Postdoctoral Research Foundation (No. 2022-ZZ-056).

Conflict of interest

The authors declare that the research was conducted in the absence of any commercial or financial relationships that could be construed as a potential conflict of interest.

Publisher's note

All claims expressed in this article are solely those of the authors and do not necessarily represent those of their affiliated organizations, or those of the publisher, the editors and the reviewers. Any product that may be evaluated in this article, or claim that may be made by its manufacturer, is not guaranteed or endorsed by the publisher.

References

Alves, R. C., Schulte, Z. M., Luiz, M. T., Bento da Silva, P., Frem, R. C. G., Rosi, N. L., et al. (2021). Breast cancer targeting of a drug delivery system through postsynthetic modification of curcumin@N(3)-bio-MOF-100 via click chemistry. *Inorg. Chem.* 60 (16), 11739–11744. doi:10.1021/acs.inorgchem.1c00538

Bao, J., Zu, X., Wang, X., Li, J., Fan, D., Shi, Y., et al. (2020). Multifunctional Hf/Mn-TCPP metal-organic framework nanoparticles for triple-modality imaging-guided PTT/RT synergistic cancer therapy. *Int. J. Nanomedicine* 15, 7687–7702. doi:10.2147/ijn.S267321

Bieniek, A., Wiśniewski, M., Czarnecka, J., Wierzbicki, J., Ziętek, M., Nowacki, M., et al. (2021). Porphyrin based 2D-MOF structures as dual-kinetic sorafenib nanocarriers for hepatoma treatment. *Int. J. Mol. Sci.* 22 (20), 11161. doi:10.3390/ijms222011161

Carrillo-Carrión, C. (2020). Nanoscale metal-organic frameworks as key players in the context of drug delivery: evolution toward theranostic platforms. *Anal. Bioanal. Chem.* 412 (1), 37–54. doi:10.1007/s00216-019-02217-y

Chen, D., Xu, Q., Wang, W., Shao, J., Huang, W., and Dong, X. (2021). Type I photosensitizers revitalizing photodynamic oncotherapy. *Small* 17 (31), e2006742. doi:10.1002/smll.202006742

Chen, J., Zhu, Y., and Kaskel, S. (2021). Porphyrin-based metal-organic frameworks for biomedical applications. *Angew. Chem. Int. Ed. Engl.* 60 (10), 5010–5035. doi:10.1002/anie.201909880

Chen, X., Huang, Y., Chen, H., Chen, Z., Chen, J., Wang, H., et al. (2022). Augmented EPR effect post IRFA to enhance the therapeutic efficacy of arsenic loaded ZIF-8 nanoparticles on residual HCC progression. *J. Nanobiotechnology* 20 (1), 34–52. doi:10.1186/s12951-021-01161-3

Chen, Y., Liu, W., Shang, Y., Cao, P., Cui, J., Li, Z., et al. (2019). Folic acid-nanoscale gadolinium-porphyrin metal-organic frameworks: fluorescence and magnetic resonance dual-modality imaging and photodynamic therapy in hepatocellular carcinoma. *Int. J. Nanomedicine* 14, 57–74. doi:10.2147/ijn.S177880

Chen, Z., Xie, H., Hu, M., Huang, T., Hu, Y., Sang, N., et al. (2020). Recent progress in treatment of hepatocellular carcinoma. *Am. J. Cancer Res.* 10 (9), 2993–3036.

Cheng, C., Li, C., Zhu, X., Han, W., Li, J., and Lv, Y. (2019). Doxorubicin-loaded Fe(3)O(4)-ZIF-8 nano-composites for hepatocellular carcinoma therapy. *J. Biomater. Appl.* 33 (10), 1373–1381. doi:10.1177/0885328219836540

Dai, H., Cheng, Z., Zhang, T., Wang, W., Shao, J., Wang, W., et al. (2022). Boron difluoride formazanate dye for high-efficiency NIR-II fluorescence imaging-guided cancer photothermal therapy. *Chin. Chem. Lett.* 33 (5), 2501–2506. doi:10.1016/j.cclet.2021.11.079

Ding, Y., Xu, H., Xu, C., Tong, Z., Zhang, S., Bai, Y., et al. (2020). A nanomedicine fabricated from gold nanoparticles-decorated metal-organic framework for cascade chemo/chemodynamic cancer therapy. *Adv. Sci.* 7 (17), 2001060–2001070. doi:10.1002/advs.202001060

Downes, C. A., and Marinescu, S. C. (2017). Electrocatalytic metal-organic frameworks for energy applications. *ChemSusChem* 10 (22), 4374–4392. doi:10.1002/cssc.201701420

Du, Y., Shi, X., Ma, W., Wen, P., Yu, P., Wang, X., et al. (2021). Phthalates promote the invasion of hepatocellular carcinoma cells by enhancing the interaction between Pregnane X receptor and E26 transformation specific sequence 1. *Pharmacol. Res.* 169, 105648. doi:10.1016/j.phrs.2021.105648

Farhadi, S., Riahi-Madvar, A., Sargazi, G., and Mortazavi, M. (2021). Immobilization of Lepidium draba peroxidase on a novel Zn-MOF nanostructure. *Int. J. Biol. Macromol.* 173, 366–378. doi:10.1016/j.ijbiomac.2020.12.216

Feng, G., Zhang, G. Q., and Ding, D. (2020). Design of superior phototheranostic agents guided by Jablonski diagrams. *Chem. Soc. Rev.* 49 (22), 8179–8234. doi:10.1039/d0cs00671h

Feng, Y., Gu, S., Chen, Y., Gao, X., Ren, Y., Chen, J., et al. (2020). Virtual screening and optimization of novel mTOR inhibitors for radiosensitization of

hepatocellular carcinoma. *Drug Des. devel. Ther.* 14, 1779–1798. doi:10.2147/DDDT.S249156

Fu, X., Yang, Z., Deng, T., Chen, J., Wen, Y., Fu, X., et al. (2020). A natural polysaccharide mediated MOF-based Ce6 delivery system with improved biological properties for photodynamic therapy. *J. Mat. Chem. B* 8 (7), 1481–1488. doi:10.1039/c9tb02482d

Fytory, M., Arafa, K. K., El Rouby, W. M. A., Farghali, A. A., Abdel-Hafiez, M., and El-Sherbiny, I. M. (2021). Dual-ligated metal organic framework as novel multifunctional nanovehicle for targeted drug delivery for hepatic cancer treatment. *Sci. Rep.* 11 (1), 19808. doi:10.1038/s41598-021-99407-5

Gharehdaghi, Z., Rahimi, R., Naghib, S. M., and Molaabasi, F. (2021). Cu (II)-porphyrin metal-organic framework/graphene oxide: synthesis, characterization, and application as a pH-responsive drug carrier for breast cancer treatment. *J. Biol. Inorg. Chem.* 26 (6), 689–704. doi:10.1007/s00775-021-01887-3

Hao, X., Sun, G., Zhang, Y., Kong, X., Rong, D., Song, J., et al. (2021). Targeting immune cells in the tumor microenvironment of HCC: New opportunities and challenges. *Front. Cell Dev. Biol.* 9, 775462–775480. doi:10.3389/fcell.2021.775462

Hao, Y. N., Qu, C. C., Shu, Y., Wang, J. H., and Chen, W. (2021). Construction of novel nanocomposites (Cu-MOF/GOD@HA) for chemodynamic therapy. *Nanomater. (Basel)* 11 (7), 1843–1855. doi:10.3390/nano11071843

He, M., Chen, Y., Tao, C., Tian, Q., An, L., Lin, J., et al. (2019). Mn-Porphyrin-Based metal-organic framework with high longitudinal relaxivity for magnetic resonance imaging guidance and oxygen self-supplementing photodynamic therapy. *ACS Appl. Mat. Interfaces* 11 (45), 41946–41956. doi:10.1021/acsami.9b15083

Huang, X., Sun, X., Wang, W., Shen, Q., Shen, Q., Tang, X., et al. (2021). Nanoscale metal-organic frameworks for tumor phototherapy. *J. Mat. Chem. B* 9 (18), 3756–3777. doi:10.1039/d1tb00349f

Jayaramulu, K., Horn, M., Schneemann, A., Saini, H., Bakandritsos, A., Ranc, V., et al. (2021). Covalent graphene-MOF hybrids for high-performance asymmetric supercapacitors. *Adv. Mat.* 33 (4), 2004560–2004570. doi:10.1002/adma.202004560

Jiang, Q., Zhang, M., Sun, Q., Yin, D., Xuan, Z., and Yang, Y. (2021). Enhancing the antitumor effect of doxorubicin with photosensitive metal-organic framework nanoparticles against breast cancer. *Mol. Pharm.* 18 (8), 3026–3036. doi:10.1021/acs.molpharmaceut.1c00249

Jing, Z., Wang, X., Li, N., Sun, Z., Zhang, D., Zhou, L., et al. (2021). Ultrasound-guided percutaneous metal-organic frameworks based codelivery system of doxorubicin/acetazolamide for hepatocellular carcinoma therapy. *Clin. Transl. Med.* 11 (10), 600–606. doi:10.1002/ctm2.600

Lakshmi, B. A., and Kim, S. (2019). Current and emerging applications of nanostructured metal-organic frameworks in cancer-targeted theranostics. *Mat. Sci. Eng. C Mat. Biol. Appl.* 105, 110091–110102. doi:10.1016/j.msec.2019.110091

Lan, G., Ni, K., Xu, Z., Veroneau, S. S., Song, Y., and Lin, W. (2018). Nanoscale metal-organic framework overcomes hypoxia for photodynamic therapy primed cancer immunotherapy. *J. Am. Chem. Soc.* 140 (17), 5670–5673. doi:10.1021/jacs.8b01072

Lawson, H. D., Walton, S. P., and Chan, C. (2021). Metal-organic frameworks for drug delivery: A design perspective. *ACS Appl. Mat. Interfaces* 13 (6), 7004–7020. doi:10.1021/acsami.1c01089

Li, B., Wang, X., Chen, L., Zhou, Y., Dang, W., Chang, J., et al. (2018). Ultrathin Cu-TCPP MOF nanosheets: a new theragnostic nanoplatform with magnetic resonance/near-infrared thermal imaging for synergistic phototherapy of cancers. *Theranostics* 8 (15), 4086–4096. doi:10.7150/thno.25433

Li, T., Cui, P., and Sun, D. (2022). Uncoordinated hexafluorosilicates in a microporous metal-organic framework enabled C(2)H(2)/CO(2) separation. *Inorg. Chem.* 61 (10), 4251–4256. doi:10.1021/acs.inorgchem.2c00409

Li, Z., Yang, G., Wang, R., Wang, Y., Wang, J., Yang, M., et al. (2022). γ-Cyclodextrin metal-organic framework as a carrier to deliver triptolide for the treatment of hepatocellular carcinoma. *Drug Deliv. Transl. Res.* 12 (5), 1096–1104. doi:10.1007/s13346-021-00978-7

Liu, L., Zhuang, J., Tan, J., Liu, T., Fan, W., Zhang, Y., et al. (2022). Doxorubicin-loaded UiO-66/Bi(2)S(3) nanocomposite-enhanced synergistic transarterial chemoembolization and photothermal therapy against hepatocellular carcinoma. *ACS Appl. Mat. Interfaces* 14 (6), 7579–7591. doi:10.1021/acsami.1c19121

Liu, W., Wang, Y. M., Li, Y. H., Cai, S. J., Yin, X. B., He, X. W., et al. (2017). Fluorescent imaging-guided chemotherapy-and-photodynamic dual therapy with nanoscale porphyrin metal-organic framework. *Small* 13 (17), 1603459. doi:10.1002/smll.201603459

Liu, X., Liang, T., Zhang, R., Ding, Q., Wu, S., Li, C., et al. (2021a). Iron-based metal-organic frameworks in drug delivery and biomedicine. *ACS Appl. Mat. Interfaces* 13 (8), 9643–9655. doi:10.1021/acsami.0c21486

Liu, X., Zhu, X., Qi, X., Meng, X., and Xu, K. (2021b). Co-administration of iRGD with sorafenib-loaded iron-based metal-organic framework as a targeted ferroptosis agent for liver cancer therapy. *Int. J. Nanomedicine* 16, 1037–1050. doi:10.2147/ijn.S292528

Luo, T., Nash, G. T., Xu, Z., Jiang, X., Liu, J., and Lin, W. (2021). Nanoscale metal–organic framework confines zinc-phthalocyanine photosensitizers for enhanced photodynamic therapy. *J. Am. Chem. Soc.* 143 (34), 13519–13524. doi:10.1021/jacs.1c07379

Ma, Y., Qu, X., Liu, C., Xu, Q., and Tu, K. (2021). Metal-organic frameworks and their composites towards biomedical applications. *Front. Mol. Biosci.* 8, 805228–805252. doi:10.3389/fmolb.2021.805228

Mao, D., Xu, M., Jiang, Q., Sun, H., Sun, F., Yang, R., et al. (2022). A single nucleotide mixture enhances the antitumor activity of molecular-targeted drugs against hepatocellular carcinoma. *Front. Pharmacol.* 13, 951831. doi:10.3389/fphar.2022.951831

Neufeld, M. J., Lutzke, A., Pratx, G., and Sun, C. (2021). High-Z metal-organic frameworks for X-ray radiation-based cancer theranostics. *Chemistry* 27 (10), 3229–3237. doi:10.1002/chem.202003523

Osterrieth, J. W. M., and Fairen-Jimenez, D. (2021). Metal-organic framework composites for theragnostics and drug delivery applications. *Biotechnol. J.* 16 (2), 2000005–2000019. doi:10.1002/biot.202000005

Philips, C. A., Rajesh, S., Nair, D. C., Ahamed, R., Abduljaleel, J. K., and Augustine, P. (2021). Hepatocellular carcinoma in 2021: An exhaustive update. *Cureus* 13 (11), 19274–19293. doi:10.7759/cureus.19274

Qin, J. H., Zhang, H., Sun, P., Huang, Y. D., Shen, Q., Yang, X. G., et al. (2020). Ionic liquid induced highly dense assembly of porphyrin in MOF nanosheets for photodynamic therapy. *Dalton Trans.* 49 (48), 17772–17778. doi:10.1039/d0dt03031g

Rao, D., Wang, B., Zhong, H., Yan, Y., and Ding, C. F. (2022). Construction of boric acid-functionalized metal-organic frameworks for glycopeptide recognition in the serum of cervical cancer patients. *Rapid Commun. Mass Spectrom.* 36 (13), 9314–9320. doi:10.1002/rcm.9314

Rinaldi, L., Vetrano, E., Rinaldi, B., Galiero, R., Caturano, A., Salvatore, T., et al. (2021). HCC and molecular targeting therapies: Back to the future. *Biomedicines* 9 (10), 1345–1363. doi:10.3390/biomedicines9101345

Sadeghi, N., and Sillanpää, M. (2021). High selective photocatalytic CO(2) conversion into liquid solar fuel over a cobalt porphyrin-based metal-organic framework. *Photochem. Photobiol. Sci.* 20 (3), 391–399. doi:10.1007/s43630-021-00027-9

Samui, A., Pal, K., Karmakar, P., and Sahu, S. K. (2019). *In situ* synthesized lactobionic acid conjugated NMOFs, a smart material for imaging and targeted drug delivery in hepatocellular carcinoma. *Mat. Sci. Eng. C Mat. Biol. Appl.* 98, 772–781. doi:10.1016/j.msec.2019.01.032

Sava Gallis, D. F., Rohwer, L. E. S., Rodriguez, M. A., Barnhart-Dailey, M. C., Butler, K. S., Luk, T. S., et al. (2017). Multifunctional, tunable metal-organic framework materials platform for bioimaging applications. *ACS Appl. Mat. Interfaces* 9 (27), 22268–22277. doi:10.1021/acsami.7b05859

Shang, Y., Zhang, H., Cheng, Y., Cao, P., Cui, J., Yin, X., et al. (2022). Fluorescent imaging-guided chemo- and photodynamic therapy of hepatocellular carcinoma with HCPT@NMOFs-RGD nanocomposites. *Int. J. Nanomedicine* 17, 1381–1395. doi:10.2147/ijn.S353803

Shi, Z., Chu, C., Zhang, Y., Su, Z., Lin, H., Pang, X., et al. (2018). Self-assembled metal-organic nanoparticles for multimodal imaging-guided photothermal therapy of hepatocellular carcinoma. *J. Biomed. Nanotechnol.* 14 (11), 1934–1943. doi:10.1166/jbn.2018.2636

Sun, Q. X., Wei, X., Zhang, S. Q., Chen, M. L., Yang, T., Yu, Y. L., et al. (2021). Dual-mode imaging of copper transporter 1 in HepG2 cells by hyphenating confocal laser scanning microscopy with laser ablation ICPMS. *Anal. Bioanal. Chem.* 413 (5), 1353–1361. doi:10.1007/s00216-020-03097-3

Sun, X., He, G., Xiong, C., Wang, C., Lian, X., Hu, L., et al. (2021). One-pot fabrication of hollow porphyrinic MOF nanoparticles with ultrahigh drug loading toward controlled delivery and synergistic cancer therapy. *ACS Appl. Mat. Interfaces* 13 (3), 3679–3693. doi:10.1021/acsami.0c20617

Tian, H., Zhang, M., Jin, G., Jiang, Y., and Luan, Y. (2021). Cu-MOF chemodynamic nanoplatform via modulating glutathione and H(2)O(2) in tumor microenvironment for amplified cancer therapy. *J. Colloid Interface Sci.* 587, 358–366. doi:10.1016/j.jcis.2020.12.028

Wan, Y., Chen, X. M., Zhang, Q., Jiang, H. B., and Feng, R. (2021). A luminescent Zn-MOF exhibiting high water stability: selective detection of Cr(VI) ion and treatment activity on sepsis. *Des. Monomers Polym.* 24 (1), 216–223. doi:10.1080/15685551.2021.1953239

Wang, C., Xiong, C., Li, Z., Hu, L., Wei, J., and Tian, J. (2021). Defect-engineered porphyrinic metal-organic framework nanoparticles for targeted multimodal

cancer phototheranostics. *Chem. Commun.* 57 (33), 4035–4038. doi:10.1039/d0cc07903k

Wang, L., Qu, X., Zhao, Y., Weng, Y., Waterhouse, G. I. N., Yan, H., et al. (2019). Exploiting single atom iron centers in a porphyrin-like MOF for efficient cancer phototherapy. *ACS Appl. Mat. Interfaces* 11 (38), 35228–35237. doi:10.1021/acsami.9b11238

Xia, J., Xue, Y., Lei, B., Xu, L., Sun, M., Li, N., et al. (2021). Multimodal channel cancer chemotherapy by 2D functional gadolinium metal-organic framework. *Natl. Sci. Rev.* 8 (7), 221–231. doi:10.1093/nsr/nwaa221

Xiao, Y., Huang, W., Zhu, D., Wang, Q., Chen, B., Liu, Z., et al. (2020). Cancer cell membrane-camouflaged MOF nanoparticles for a potent dihydroartemisinin-based hepatocellular carcinoma therapy. *RSC Adv.* 10 (12), 7194–7205. doi:10.1039/c9ra09233a

Xie, B. R., Yu, Y., Liu, X. H., Zeng, J. Y., Zou, M. Z., Li, C. X., et al. (2021). A near infrared ratiometric platform based π-extended porphyrin metal-organic framework for O(2) imaging and cancer therapy. *Biomaterials* 272, 120782–120794. doi:10.1016/j.biomaterials.2021.120782

Xiong, R., Hua, D., Van Hoeck, J., Berdecka, D., Léger, L., De Munter, S., et al. (2021). Photothermal nanofibres enable safe engineering of therapeutic cells. *Nat. Nanotechnol.* 16 (11), 1281–1291. doi:10.1038/s41565-021-00976-3

Xu, X., Chen, Y., Zhang, Y., Yao, Y., and Ji, P. (2020). Highly stable and biocompatible hyaluronic acid-rehabilitated nanoscale MOF-Fe(2+) induced ferroptosis in breast cancer cells. *J. Mat. Chem. B* 8, 9129–9138. doi:10.1039/d0tb01616k

Yang, M., Cao, S., Sun, X., Su, H., Li, H., Liu, G., et al. (2020). Self-assembled naphthalimide conjugated porphyrin nanomaterials with D–A structure for PDT/PTT synergistic therapy. *Bioconjug. Chem.* 31 (3), 663–672. doi:10.1021/acs.bioconjchem.9b00819

Yao, X., Chen, D., Zhao, B., Yang, B., Jin, Z., Fan, M., et al. (2022). Acid-degradable hydrogen-generating metal-organic framework for overcoming cancer resistance/metastasis and off-target side effects. *Adv. Sci.* 9 (10), 2101965–2101979. doi:10.1002/advs.202101965

Yu, W., Zhen, W., Zhang, Q., Li, Y., Luo, H., He, J., et al. (2020). Porphyrin-based metal-organic framework compounds as promising nanomedicines in photodynamic therapy. *ChemMedChem* 15 (19), 1766–1775. doi:10.1002/cmdc.202000353

Zeng, L., Huang, L., Wang, Z., Wei, J., Huang, K., Lin, W., et al. (2021). Self-assembled metal-organic framework stabilized organic cocrystals for biological phototherapy. *Angew. Chem. Int. Ed. Engl.* 60, 23569–23573. doi:10.1002/anie.202108076

Zhang, D., Ye, Z., Wei, L., Luo, H., and Xiao, L. (2019). Cell membrane-coated porphyrin metal-organic frameworks for cancer cell targeting and O(2)-evolving photodynamic therapy. *ACS Appl. Mat. Interfaces* 11 (43), 39594–39602. doi:10.1021/acsami.9b14084

Zhang, H., Zhang, Q., Liu, C., and Han, B. (2019). Preparation of a one-dimensional nanorod/metal organic framework Janus nanoplatform via side-specific growth for synergistic cancer therapy. *Biomater. Sci.* 7 (4), 1696–1704. doi:10.1039/c8bm01591k

Zhang, Y., Zhong, R. L., Lu, M., Wang, J. H., Jiang, C., Gao, G. K., et al. (2021). Single metal site and versatile transfer channel merged into covalent organic frameworks facilitate high-performance Li-CO(2) batteries. *ACS Cent. Sci.* 7 (1), 175–182. doi:10.1021/acscentsci.0c01390

Zhao, Q. G., Wang, J., Zhang, Y. P., Zhang, J., Tang, A. N., and Kong, D. M. (2018). A ZnO-gated porphyrinic metal-organic framework-based drug delivery system for targeted bimodal cancer therapy. *J. Mat. Chem. B* 6 (47), 7898–7907. doi:10.1039/c8tb02663g

Zhao, Y., Zhang, L., Chen, Z., Zheng, B., Ke, M., Li, X., et al. (2021). Nanostructured phthalocyanine assemblies with efficient synergistic effect of type I photoreaction and photothermal action to overcome tumor hypoxia in photodynamic therapy. *J. Am. Chem. Soc.* 143 (34), 13980–13989. doi:10.1021/jacs.1c07479

Zheng, S., Ni, J., Li, Y., Lu, M., Yao, Y., Guo, H., et al. (2021). 2-Methoxyestradiol synergizes with Erlotinib to suppress hepatocellular carcinoma by disrupting the PLAGL2-EGFR-HIF-1/2α signaling loop. *Pharmacol. Res.* 169, 105685. doi:10.1016/j.phrs.2021.105685

Zhou, Z., Zhao, J., Di, Z., Liu, B., Li, Z., Wu, X., et al. (2021). Core-shell gold nanorod@mesoporous-MOF heterostructures for combinational phototherapy. *Nanoscale* 13 (1), 131–137. doi:10.1039/d0nr07681c